Structure, morphology and electrochemical properties of $LiNi_{0.5}Mn_{0.5-x}Co_xO_2$ prepared by solid state reaction

Decheng Li [a], Yuki Sasaki [b], Masaya Kageyama [b],
Koichi Kobayakawa [b], Yuichi Sato [b,*]

[a] *High-Tech Research Center, Kanagawa University, 3-27-1 Rokkakubashi, Yokohama 221-8686, Japan*
[b] *Department of Applied Chemistry, Faculty of Engineering, Kanagawa University, 3-27-1 Rokkakubashi,
Kanagawa-ku, Yokohama 221-8686, Japan*

Abstract

A series of $LiNi_{0.5}Mn_{0.5-x}Co_xO_2$ ($0 \leq x \leq 0.5$) compounds was prepared by a solid state reaction, and their structural, morphological and electrochemical characteristics were also investigated. Co doping suppresses the formation of the impurity phase, NiO, and improves the crystallinity of the compounds. Moreover, the unequilavent substitution of cobalt for manganese would give rise to the increase in the average valence of nickel, thereby shrinkage in the lattice volume and improvement of the electrochemical properties. $LiNi_{0.5}Mn_{0.2}Co_{0.3}O_2$ shows a high reversible capacity as well as an excellent rate capability in 3–4.6 V.
© 2005 Elsevier B.V. All rights reserved.

Keywords: Li-ion battery; Cathode material; $LiNi_{0.5}Mn_{0.5-x}Co_xO_2$; Unequivalent substitution; Electrochemical behavior

1. Introduction

LiCoO$_2$ is one of the predominant cathode materials used in commercial lithium and lithium-ion batteries. Due to the relatively high cost and toxicity of cobalt, many efforts have been made to develop new materials as alternatives to LiCoO$_2$. Layered $LiNi_{0.5}Mn_{0.5}O_2$ is of great interest as a promising cathode material for lithium secondary batteries because of its high reversible capacity (about $200\,mAh\,g^{-1}$ in the voltage range of 2.5–4.5 V), good cyclic performance as well as excellent thermal stability [1–5]. It was first reported by Spahr et al. [1] and re-proposed by Ohzuku et al. [2,3] and Dahn and co-workers [4,5]. Although it had been regarded as a one-to-one mixture of LiNiO$_2$ and LiMnO$_2$, the valences of nickel and manganese have been determined to be +2 and +4, respectively [6], different from those in LiNiO$_2$ (Ni is trivalent) and LiMnO$_2$ (Mn is trivalent). How-

ever, one of its drawbacks is its lower electronic conductivity, which dramatically reduces its specific capacity even at a moderate current density [7]. It has been reported that layered $LiNi_{1/3}Mn_{1/3}Co_{1/3}O_2$ exhibited a good rate capability as well as a high reversible capacity [8–10]. This reminds us that cobalt doping in $LiNi_{0.5}Mn_{0.5}O_2$ may improve the electrochemical properties of $LiNi_{0.5}Mn_{0.5}O_2$ since $LiNi_{1/3}Mn_{1/3}Co_{1/3}O_2$ can be considered as a compound of the cobalt substituted $LiNi_{0.5}Mn_{0.5}O_2$. Several groups [11–16] have investigated the structural, morphological and electrochemical properties of $LiNi_{0.5-x}Mn_{0.5-x}Co_{2x}O_2$, and the decrease in the area specific impedance (ASI) [11] as well as improvement in the rate capability was reported [12,13]. For $LiNi_{0.5-x}Mn_{0.5-x}Co_{2x}O_2$, there is no charge compensation because one Ni^{2+} ion and one Mn^{4+} ion were presumably substituted with two Co^{3+} ions. If one Mn^{4+} ion is replaced by a Co^{3+} ion, charge compensation will occur, which would result in the formation of an oxygen deficiency or mixed Ni^{3+}/Ni^{2+}. It is well known that the existence of mixed-valent cations significantly contributes to the inherent electronic conductivity of electrodes during charge and

* Corresponding author. Tel.: +81 45 481 5661x3885;
fax: +81 45 413 9770.

E-mail address: satouy01@kanagawa-u.ac.jp (Y. Sato).

discharge [17]. As a matter of fact, an improved electronic conductivity was observed in $LiCo_{1-x}Mg_xO_2$ due to the creation of a compensating hole [18]. Therefore, it is necessary to study the structural and electrochemical properties of $LiNi_{0.5}Mn_{0.5-x}M_xO_2$ in which the valence of M is different from tetravalent.

In the present study, $LiNi_{0.5}Mn_{0.5-x}Co_xO_2$ ($0 < x < 0.5$) compounds were prepared by a solid state reaction and their structural, morphological and electrochemical characteristics were investigated.

2. Experimental

Stoichiometric $Ni(OH)_2$ (Wako), $Mn(CH_3COO)_2 \cdot 4H_2O$ (Wako) and CoO (Wako) were dispersed into acetone and thoroughly mixed. The obtained mixtures were attempted to pre-heat at 450 °C for 6 h in air, N_2 and O_2. After being ground, the resulting precursors were mixed with stoichiometric $LiOH \cdot H_2O$ (Kishida) and pressed into pellets. These pellets were sintered at 950 °C for 25 h in O_2 and then cooled to room temperature in the furnace. We found that the final products show the lowest impurities content in terms of their XRD profiles if their precursor were treated in N_2. So, we just provided their results in this work.

The XRD measurements were carried out using a Rigaku Rint1000 diffractometer equipped with a monochromator and Cu target tube.

The scanning electron microscope (SEM) study of the samples was performed by Hitachi S-4000 electron microscope.

The charge/discharge tests were carried out using the CR2032 coin-type cell, which consists of a cathode and lithium metal anode separated by a Celgard 2400 porous polypropylene film. The cathode contains a mixture of 20 mg of accurately weigh active materials and 13 mg of the teflonized acetylene black (TAB-2) as the conducting binder. The mixture was pressed onto a stainless mesh and dried at 130 °C for 5 h. The cells were assembled in a glove box filled with dried argon gas. The electrolyte is 1 M $LiPF_6$ in ethylene carbonate/dimethyl carbonate (EC/DMC, 1:2 by volume).

A cyclic voltammetry study was carried out using a homemade tri-electrode cell, using metallic lithium as the counter and reference electrodes and 1 M $LiPF_6$ in ethylene carbonate/dimethyl carbonate (EC/DMC, 1:2 in volume) as the electrolyte. Three milligrams of the active material was well mixed with 2 mg TAB-2 and pressed onto a stainless mesh with an area of about 0.75 cm^2. The cell was operated at a scan rate of 0.05 mV s^{-1} in the voltage range of 3–4.6 V versus Li/Li^+.

3. Results and discussion

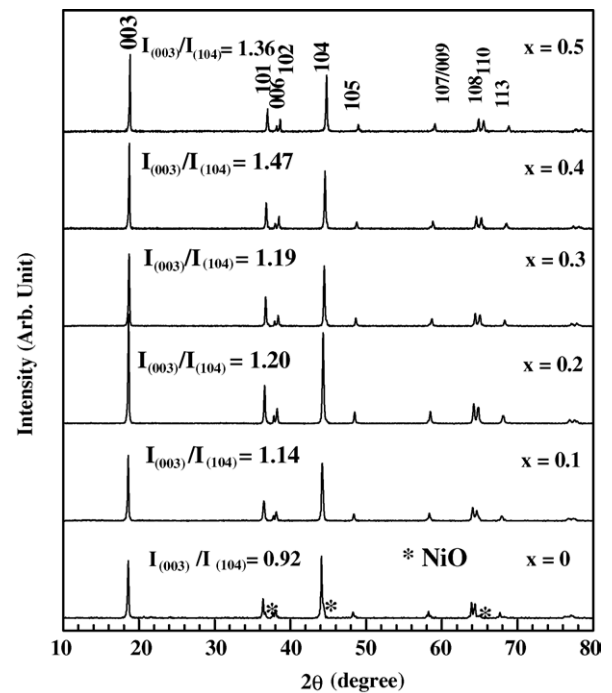The color of the as-prepared $LiNi_{0.5}Mn_{0.5}O_2$ is dark-brown whereas the colors of the $LiNi_{0.5}Mn_{0.5-x}Co_xO_2$

Fig. 1. XRD patterns of $LiNi_{0.5}Mn_{0.5-x}Co_xO_2$ compounds prepared at 950 °C.

compounds are black, implying that cobalt substitution for manganese induces some changes in the energy level of the $LiNi_{0.5}Mn_{0.5}O_2$. Fig. 1 shows the XRD patterns of $LiNi_{0.5}Mn_{0.5-x}Co_xO_2$. An impurity phase, NiO, was ob-
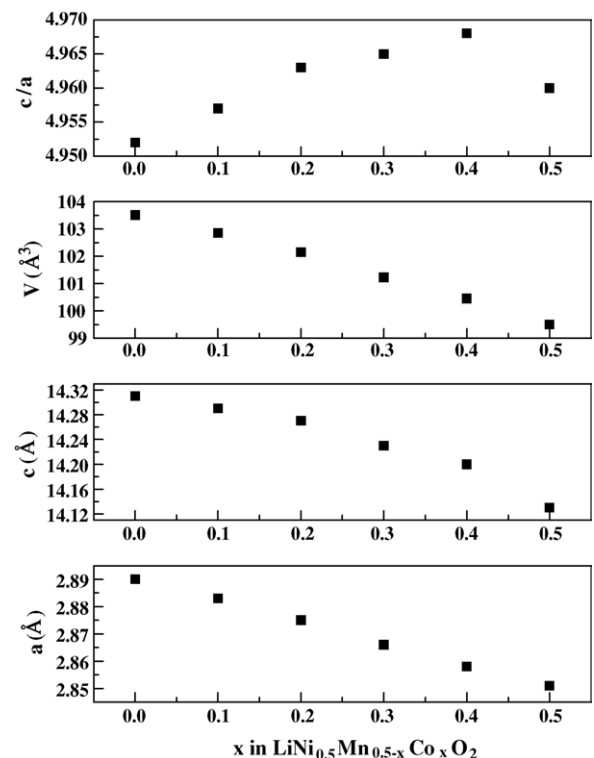
Fig. 2. Lattice parameters vs. x in $LiNi_{0.5}Mn_{0.5-x}Co_xO_2$ compounds.

served in $LiNi_{0.5}Mn_{0.5}O_2$, which is related to the preferential formation of Li_2MnO_3 to $LiNiO_2$ [19]. However, its diffraction peaks disappear in the $LiNi_{0.5}Mn_{0.5-x}Co_xO_2$ compounds with $x \geq 0.1$, suggesting that the substitution of Co for Mn can promote the formation of $LiNi_{0.5}Mn_{0.5-x}Co_xO_2$. Moreover, the $LiNi_{0.5}Mn_{0.5-x}Co_xO_2$ compounds have a layered structure in terms of their XRD profiles and all peaks can be indexed on the basis of the α-$NaFeO_2$ structure (space group $R\bar{3}m$). As the cobalt content, x, increases, both (0 0 3) and (1 1 0) peaks shift to a higher angle, indicating that cobalt doping shrinks the lattice along both a and c axes. Moreover, the splitting between (1 0 8) and (1 1 0) peaks becomes clear. As illustrated in Fig. 1, the intensity ration of I_{003}/I_{104} increased after the cobalt doping. Since this ratio is sensitive to the degree of cation mixing [20], this result suggests that cobalt doping seems to suppress the occurrence of cation mixing.

The lattice parameters of the $LiNi_{0.5}Mn_{0.5-x}Co_xO_2$ compounds were roughly calculated and the results are illustrated in Fig. 2. The lattice parameters for $LiNi_{0.5}Mn_{0.5}O_2$ are $a = 2.89$ Å and $c = 14.31$ Å, quite consistent with Ohzuku's reported results [2]. As the cobalt content increases, the lattice parameter, a, decreases monotonously while the lattice parameter, c, gradually decreases from 14.31 Å for $x = 0$ to 14.19 Å for $x = 0.4$ and then down to 14.13 Å for $x = 0.5$. The cell volume decreases from 103.51 Å^3 for $LiNi_{0.5}Mn_{0.5}O_2$ to 99.49 Å^3 for $LiNi_{0.5}Co_{0.5}O_2$; this shrinkage is about 4%. It is well known that the radius of Co^{3+} (0.545 Å) is slightly larger than that of Mn^{4+} (0.53 Å) while smaller than that of Ni^{2+} (0.69 Å) [15]. Moreover, the valences of Ni and Co in $LiNi_{0.5}Co_{0.5}O_2$ are both trivalent. Thus, we believed that the shrinkage in the lattice parameters should be ascribed to the decrease in the Ni^{2+} content. The trigonal distortion, c/a, gradually increases from 4.95 for $x = 0$ to 4.96 for $x = 0.5$, quite consistent with Ohzuku's reported results [21]. This indicates that the substitution of cobalt for manganese promotes the formation of a layered structure.

SEM photographs of $LiNi_{0.5}Mn_{0.5-x}Co_xO_2$ prepared at 950 °C were provided in Fig. 3. $LiNi_{0.5}Mn_{0.5}O_2$ has an agglomerated morphology and the size of the primary parti-
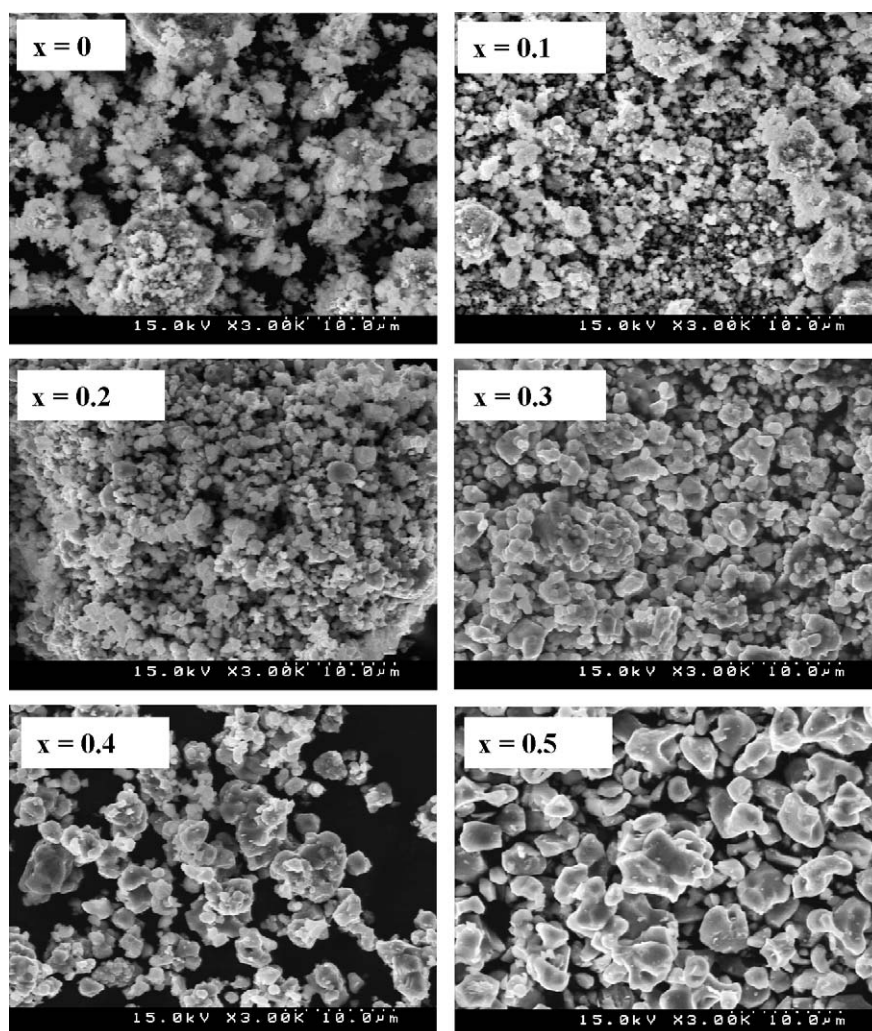

Fig. 3. SEM photographs of $LiNi_{0.5}Mn_{0.5-x}Co_xO_2$ compounds.

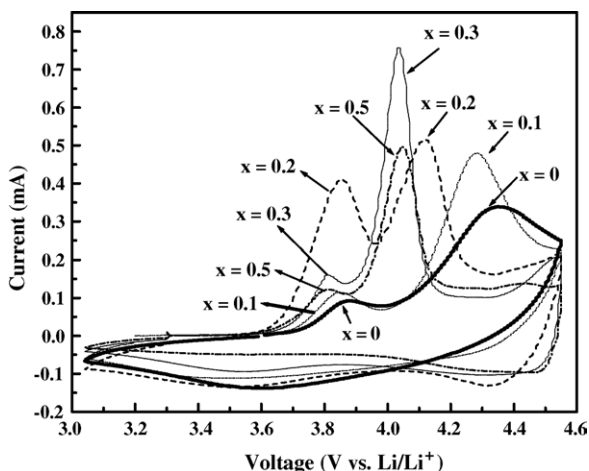Fig. 4. Cyclic voltammograms of $LiNi_{0.5}Mn_{0.5-x}Co_xO_2$ compounds operated from 3 to 4.6 V at a scan rate of $0.05\,mV\,s^{-1}$.

cle is on a nano-scale. As the cobalt content increases, the morphologies of the particles become well shaped with an enlarged size. Moreover, there is a relatively homogeneous size distribution. The average particle size for $x \geq 0.2$ is about 1–2 μm. These results suggest that Co doping improves the crystallinity of the $LiNi_{0.5}Mn_{0.5-x}Co_xO_2$ compounds.

Fig. 4 are cyclic voltammograms of the $LiNi_{0.5}Mn_{0.5-x}Co_xO_2$ compounds operated from 3 to 4.6 V at a scan rate of $0.05\,mV\,s^{-1}$. Two anodic peaks were observed in $LiNi_{0.5}Mn_{0.5}O_2$. One is at about 3.86 V (peak 1) and the other is at about 4.35 V (peak 2). Since Arachi et al. [22] reported that the divalent nickel was oxidized to trivalent after charging, we ascribe peak 1 to Ni^{2+}/Ni^{3+} redox couple while attributing peak 2 to the Ni^{3+}/Ni^{4+} redox couple. As the cobalt content increases, the peak potential, E_{p1} slightly shifts to a lower value while E_{p2} dramatically changes. Moreover, the shapes of both peak 1 and peak 2 become sharp, implying that Co doping improves the kinetic properties of the $LiNi_{0.5}Mn_{0.5-x}Co_xO_2$ compounds.

Table 1
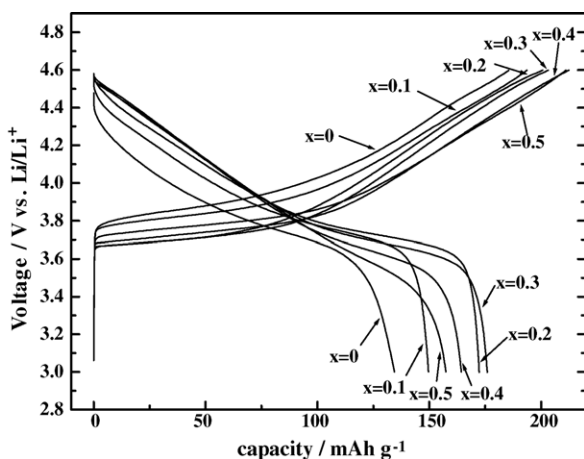The initial charge/discharge capacities as well as irreversible capacity of the $LiNi_{0.5}Mn_{0.5-x}Co_xO_2$ compounds

x	1st charge (mAh g^{-1})	1st discharge (mAh g^{-1})	Irreversible capacity (mAh g^{-1})
0.0	185	134	51
0.1	193	149	44
0.2	211	172	39
0.3	212	176	36
0.4	203	164	39
0.5	200	157	43

Fig. 5 shows the initial charge–discharge curves of the $LiNi_{0.5}Mn_{0.5-x}Co_xO_2$ compounds operated at a current density of $0.4\,mA\,cm^{-2}$ ($40\,mA\,g^{-1}$) from 3 to 4.6 V. All samples are the same in terms of the shape of their charge/discharge curves and no new plateau is observed. It is noted that the polarization of the cells declines as the cobalt content increases. Since the polarization of a cell is closely related to its internal resistance, we believe that cobalt doping would be helpful in decreasing the charge transfer resistance. Furthermore, the cobalt substitution for manganese increases both the initial charge and discharge capacities and decreases the irreversible capacity, as illustrated in Table 1. However, when the cobalt content, x, is over 0.3, both the initial charge and discharge capacities slightly decrease while irreversible capacity increases slightly. This is probably related to the reduction in the Ni^{2+} content as well as the larger particle size for $x = 0.4$ and 0.5.

The rate capability of the $LiNi_{0.5}Mn_{0.5-x}Co_xO_2$ compounds operated in the range of 3–4.6 V is illustrated in Fig. 6. Cells were charged at a current density of $0.1\,mA\,cm^{-2}$ and discharged at 0.1, 0.2, 0.4, 0.8, 1.6 and $3.2\,mA\,cm^{-2}$ in the 1st, 2nd, 3rd, 4th, 5th and 6th cycles, respectively. Co doping can significantly improve the rate capability, and $LiNi_{0.5}Mn_{0.2}Co_{0.3}O_2$ exhibits the best rate performance.

Fig. 5. Initial charge–discharge curves of $LiNi_{0.5}Mn_{0.5-x}Co_xO_2$ compounds operated at a current density of $0.4\,mA\,cm^{-2}$ ($40\,mA\,g^{-1}$) from 3 to 4.6 V.

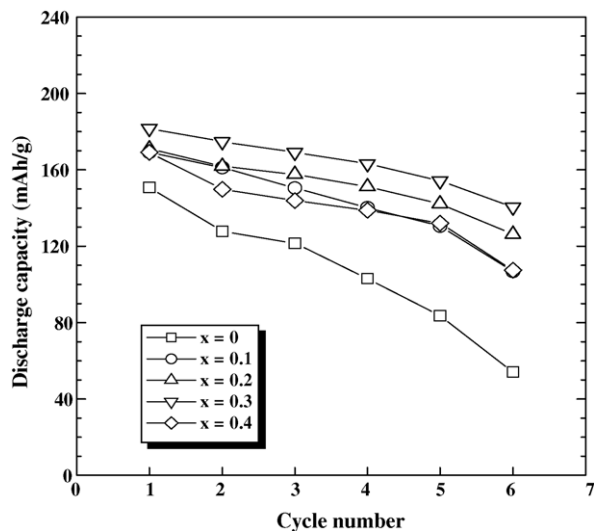Fig. 6. Rate capability of $LiNi_{0.5}Mn_{0.5-x}Co_xO_2$ compounds operated from 3 to 4.6 V.
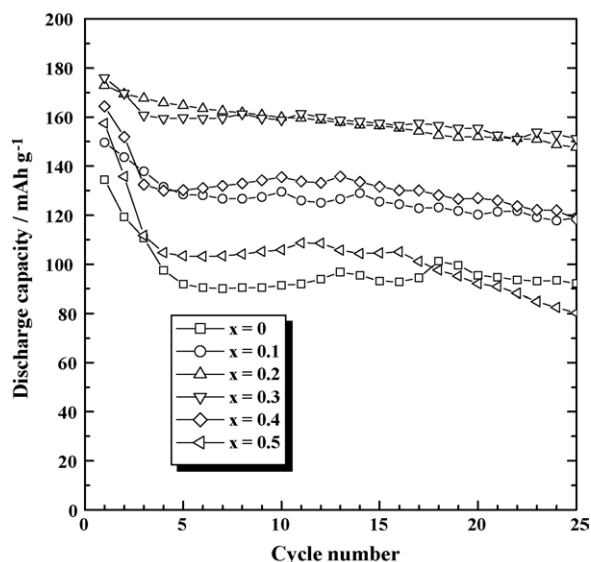
Fig. 7. Cyclic performance of $LiNi_{0.5}Mn_{0.5-x}Co_xO_2$ compounds operated from 3 to 4.6 V.

When the discharge current density increases from 0.1 to 3.2 mA cm^{-2}, the discharge capacity decreases from 181 to 140 mAh g^{-1}, about 77% of the initial discharge capacity. We believe that the upgraded rate capability results from the improved electronic conductivity due to the presence of mixed nickel in these compounds.

Fig. 7 shows the cyclic performance of the $LiNi_{0.5}Mn_{0.5-x}Co_xO_2$ compounds operated at a current density of 0.4 mA cm^{-2} (40 mA g^{-1}) at room temperature. All compounds excepting for $LiNi_{0.5}Co_{0.5}O_2$ show good cycleability in the range of 3–4.6 V. The poor cyclic performance of $LiNi_{0.5}Co_{0.5}O_2$ has been ascribed to the large change in the unit cell volume during the charge and discharge cycling [21]. Co doping significantly improves the reversible capacity. The discharge capacity of $LiNi_{0.5}Mn_{0.2}Co_{0.3}O_2$ is 151 mAh g^{-1} after 25 cycles, about 86% of its initial discharge capacity.

4. Conclusions

Due to the unequivalent substitution of cobalt for manganese in $LiNi_{0.5}Mn_{0.5}O_2$, the average valence of nickel increases in order to maintain the electric neutrality of the compound. This results in shrinkage in the lattice volume. Moreover, the increase in the reversible capacity as well as the improvement in the rate capability were also attributed to the presence of the mixed valent nickel in these compounds. These results suggest that the unequivalent substitution of foreign metal ions for Mn ions in $LiNi_{0.5}Mn_{0.5}O_2$ is an effective method to improve the electrochemical properties of $LiNi_{0.5}Mn_{0.5}O_2$.

References

[1] M.E. Spahr, P. Novak, B. Schnyder, O. Haas, R. Nesper, J. Power Sources 68 (1997) 629.
[2] T. Ohzuku, Y. Makimura, Chem. Lett. (2001) 744.
[3] Y. Makimura, T. Ohzuku, J. Power Sources 119–121 (1997) 156.
[4] Z. Lu, D.D. MacNeil, J.R. Dahn, Electrochem. Solid State Lett. 4 (2001) A191.
[5] Z. Lu, L.Y. Beaulieu, R.A. Donaberger, C.L. Thomas, J.R. Dahn, J. Electrochem. Soc. 149 (2002) A778.
[6] W.-S. Yoon, Y. Park, X.-Q. Yang, M. Balasubramanian, J. McBreen, C.P. Grey, Electrochem. Solid State Lett. 5 (2002) A263.
[7] B.L. Cushing, J.B. Goodenough, Solid State Sci. 4 (2002) 1487.
[8] T. Ohzuku, Y. Makimura, Chem. Lett. (2001) 642.
[9] K.M. Shaju, G.V. Subba Rao, B.V.R. Chowdari, Electrochim. Acta 48 (2002) 145.
[10] D. Li, T. Muta, L. Zhang, M. Yoshio, H. Noguchi, J. Power Sources 132 (2004) 150.
[11] S.-H. Kang, J. Kim, M.E. Stoll, D. Abraham, Y.K. Sun, K. Amine, J. Power Sources 112 (2002) 41.
[12] D. Li, H. Noguchi, M. Yoshio, Electrochim. Acta 50 (2004) 425.
[13] Y. Sun, C. Ouyang, Z. Wang, X. Huang, L. Chen, J. Electrochem. Soc. 151 (2004) A504.
[14] Z. Lu, D.D. MacNeil, J.R. Dahn, Electrochem. Solid State Lett. 4 (2001) A200.
[15] D.D. MacNeil, Z. Lu, J.R. Dahn, J. Electrochem. Soc. 149 (2002) A1332.
[16] S. Jouanneau, D.D. MacNeil, Z. Lu, S.D. Beattie, G. Murphy, J.R. Dahn, J. Electrochem. Soc. 150 (2003) A1299.
[17] M. Thackeray, Nature Mater. 1 (2002) 81.
[18] H. Tukamoto, A.R. West, J. Electrochem. Soc. 144 (1997) 3164.
[19] M. Yoshio, K. Todorov, K. Yamato, H. Noguchi, J. Itoh, M. Okada, T. Mouri, J. Power Sources 74 (1998) 46.
[20] T. Ohzuku, A. Ueda, M. Nagayama, J. Electrochem. Soc. 140 (1993) 1862.
[21] A. Ueda, T. Ohzuku, J. Electrochem. Soc. 141 (1994) 2013.
[22] Y. Arachi, H. Kobayashi, S. Emura, Y. Nakata, M. Tanaka, T. Asai, Chem. Lett. 32 (2003) 60.